Integrated production and separation of furfural using an acidic-based aqueous biphasic system

Eduarda S. Morais†, Nicolas Schaeffer†, Mara G. Freire†, Carmen S.R. Freire†, João A. P. Coutinho† and Armando J. D. Silvestre†**

†CICECO – Aveiro Institute of Materials, Department of Chemistry, University of Aveiro, Campus Universitário de Santiago, 3810-193 Aveiro, Portugal

Number of pages: 19

Number of figures: 11

Number of Tables: 5

Table S1. Tested conditions in the initial assays carried out in the Monowave 300 microwave.

IL (wt.%)	HCl (wt.%)	Temperature (°C)	S/L ratio	Time (min)
20, 30 and 40	5 and 10	110, 120, 130, 140, 150	0.05	1, 2, 2.5, 3 and 4

Reaction Assays Results

Furfural production assays in the ABS formed by the IL $[P_{44414}]Cl$ and HCl were initially carried out with conventional heating; however, and due to dissatisfactory furfural yields, microwave heating assays were conducted to increase furfural yield and to reduce the time of reaction, which in turn translate into lower furfural degradation.

Figure S1 reports the results of two assays conducted in the microwave reactor with fixed temperature and HCl concentration. These assays were performed to address the effect of the IL wt.% in the furfural yield and extraction efficiency to the IL-rich phase (top phase). All the assays were conducted in the biphasic region of the system, thus assuring a continuous furfural production and extraction to the IL-rich phase.

Considering that the biphasic strategy intends to separate the products to prevent undesirable side reactions, the evaluation of furfural extraction efficiency (EE%) is key. The results attained reveal the increase in both furfural yield (from 26.6 to 33.4%) and EE% (from 82.2 to 87.0%) when the IL wt.% is increased from 20 to 30 wt.%. This behavior is mostly correlated to an increase in size of the IL-rich phase, which decreases the phase saturation with furfural and thus furfural degradation in the aqueous phase.

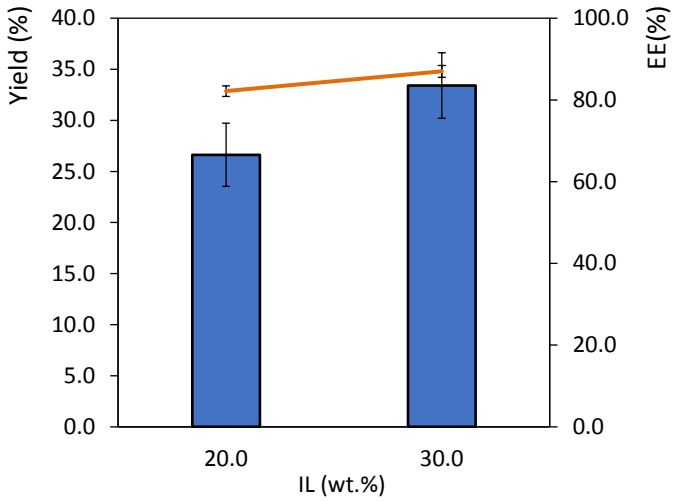

Figure S1. Furfural yield (bars) and extraction eficiency, EE (dots) in the ABS at different IL concentrations (wt.%). The HCl concentration is fixed at 5 wt.% and the temperature at 120 °C.

The results attained in these initial assays highlight the importance of the IL wt.% in furfural yield. On the other hand, temperature and reaction time display an important role in furfural yield. In this sense, we studied the temperatures of 120 and 130 °C at 2.5 and 3.0 min of reaction time, with the fixed conditions of 5 wt.% of HCl and 30 wt.% of IL (Figure S2). It was observed that the yield increases significatively, for both tested reaction times, when the temperature increases up to 130 °C. On the contrary, increasing the time does not influence the results at 120 °C, but there is a sharp increase in furfural yield, from 46.3% to 60.3%, at 130 °C. These results show the determining factor of temperature, since at 120 °C a plateau in yield was reached. Higher temperatures were also tested, beginning with 140 °C at 2.5 minutes time. However, it was visually apparent that some degradation was occurring, which was reflected in the yield attained (56.9%). Therefore, a shorter reaction time was tested (1.0 min) with higher temperatures (140 and 150 °C), attaining higher yields (77.12% and 70.16%, respectively). These last results reveal that a careful balance between temperature and time must be maintained, since a decrease in yield is observed when the temperature is increased after an established period of time, most likely due to furfural degradation.

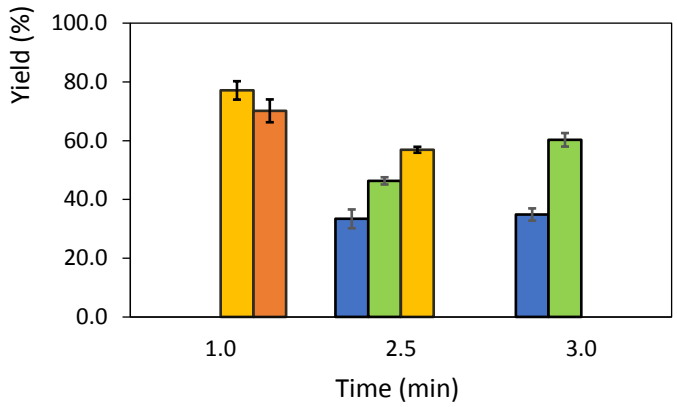

Figure S2. Furfural yield in the ABS at different temperatures (120 °C, 130 °C, 140 °C, 150 °C) and reaction times. The HCl concentration is fixed at 5 wt.% and the IL concentration is fixed at 30 wt.%.

Process optimization – response surface methodology (RSM)

In a 2^k surface response methodology there are *k* factors that contribute to a different response, and the data are treated according to a second order polynomial equation according to equation S1:

$$y = \beta_0 + \sum \beta_i X_i + \sum \beta_{ii} X_i^2 + \sum_{i<j} \beta_{ij} X_i X_j \quad \text{(S1)}$$

where y is the response variable and β_0, β_i , β_{ii} and β_{ij} are the adjusted coefficients for the intercept, linear, quadratic and interaction terms, respectively, and X_i and X_j are independent variables. This model allows the drawing of surface response curves and through their analysis the optimal conditions can be determined.[1] The 2^3 factorial planning has been defined by the central point (zero level), the factorial points (1 and −1, level one) and the axial points (level α) The axial points are encoded at a distance α from the central point, according to equation S2:

$$\alpha = (2^k)^{1/4} \quad \text{(S2)}$$

Table S2. 2^3 factorial planning.

Experiment	χ_1	χ_2	χ_3
1	-1	-1	-1
2	1	-1	-1
3	-1	1	-1
4	1	1	-1
5	-1	-1	1
6	1	-1	1
7	-1	1	1

8	1	1	1
9	-1.68	0	0
10	1.68	0	0
11	0	-1.68	0
12	0	1.68	0
13	0	0	-1.68
14	0	0	1.68
15	0	0	0
16	0	0	0
17	0	0	0
18	0	0	0
19	0	0	0
20	0	0	0

Table S3. Coded levels of independents variables used in the first and second factorial planning.

Studied parameters	Symbol	Level				
		Axial	**Factorial**	**Central**	**Factorial**	**Axial**
		-1.68	**-1**	**0**	**1**	**1.68**
HCl (wt.%)	HCl	0.8	2.5	5.0	7.5	9.2
Temperature (°C)	T	123.20	130.0	140.0	150.0	156.8
IL (wt.%)	IL	13.2	20.0	30.0	40.0	46.8

Table S4. Regression coefficients of the predicted second-order polynomial model from factorial planning for the dependable variable of furfural yield.

	Regression coefficients	Standard deviation	t-student (10)	P-value
Interception	58.1395	2.4101	24.1234	<0.05
HCl	12.2640	3.1997	3.8328	<0.05
HCl ^{2}	-20.7994	3.1184	-6.6698	<0.05
Temperature	16.9536	3.1997	5.2985	<0.05
Temperature ^{2}	-9.1409	3.1184	-2.9312	<0.05
IL	7.3026	3.1997	2.2822	<0.05
IL^2	-3.58304	3.1184	-1.1490	0.2773
HCl × Temperature	-21.7383	4.1787	-5.2021	<0.05
HCl × IL	-12.0796	4.1787	-2.8907	<0.05
IL × Temperature	-3.9928	4.1787	-0.9555	0.3618

Table S5. Regression coefficients of the predicted second-order polynomial model from factorial planning for the dependable variable of D factor.

	Regression coefficients	Standard deviation	t-student (10)	P-value
Interception	5.0928	0.54758	9.3006	<0.05
HCl	-0.3363	0.72698	-0.9252	0.37664
HCl ^{2}	-1.0352	0.70852	-2.9222	<0.05
Temperature	1.0722	0.72698	2.9497	<0.05
Temperature ^{2}	0.0597	0.70852	0.1686	0.86946
IL	1.8782	0.72698	5.1671	<0.05
IL^2	0.0318	0.70852	0.0899	0.93012
HCl × Temperature	-1.3796	0.94943	-2.9060	<0.05
HCl × IL	-0.5885	0.94943	-1.2396	0.24340
IL × Temperature	-0.5834	0.94943	-1.2290	0.24719

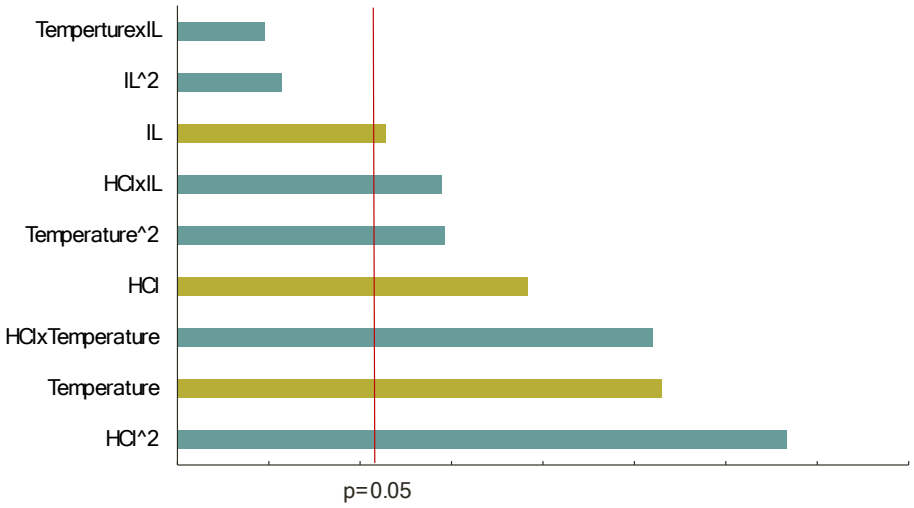

Figure S3. Pareto chart for the standardized main effects (positive (■) and negative (■)) in the factorial planning for furfural yield optimization. Vertical line indicates the statistical significance of the effects.

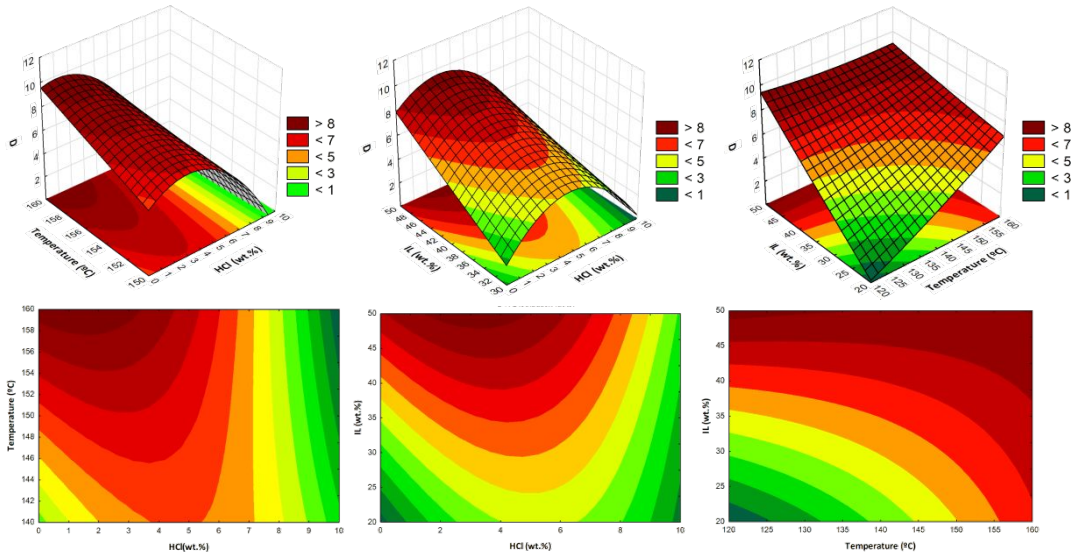

Figure S4. Response surface (top) and contour plots (bottom) of the distribution factor (D) using a biphasic system with $[P_{444(14)}]Cl$ with the combined effects of: (i) temperature and HCl concentration; (ii) IL and HCl concentrations; and (iii) IL concentration and temperature.

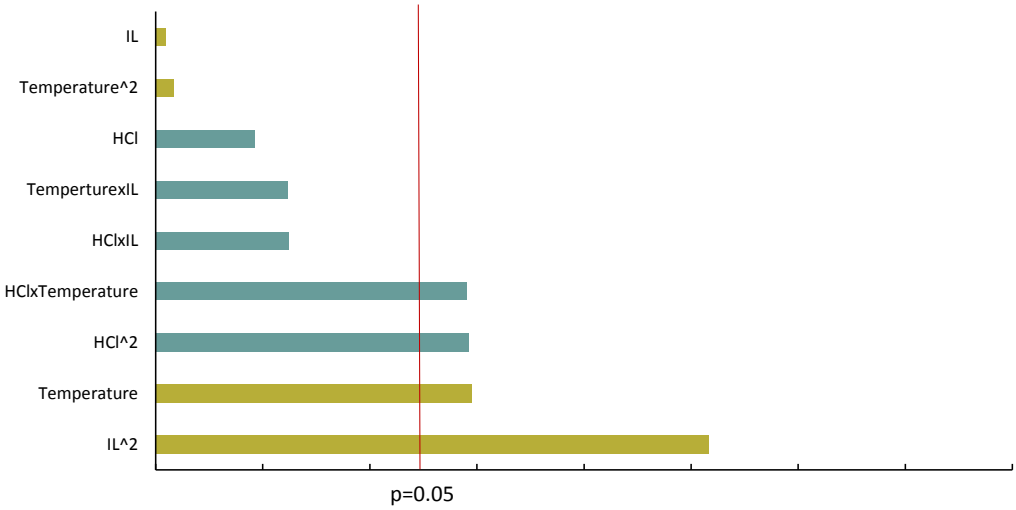

Figure S5. Pareto chart for the standardized main effects (positive (■) and negative (■)) in the factorial planning for the D factor optimization. Vertical line indicates the statistical significance of the effects.

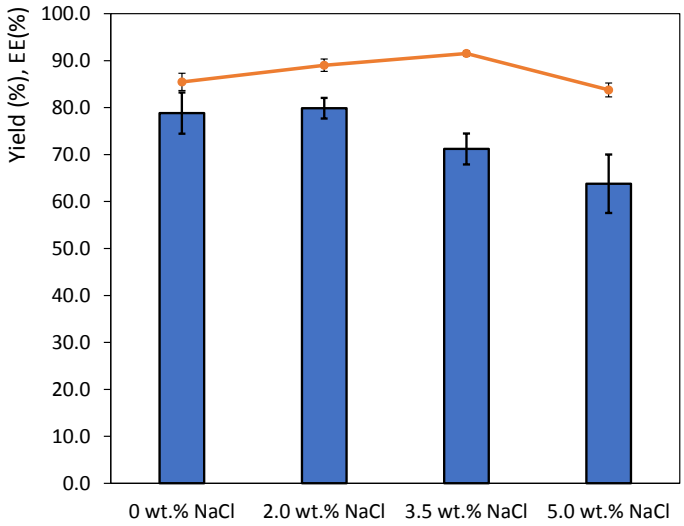

Figure S6. Furfural yield (bars) and extraction eficiency (dots) in the ABS. The values in the X axis correspond to the concentration of NaCl that substituted the fixed concentration of 6.5 wt.% of HCl. The assays were conducted in the fixed conditions of 140 °C and 30 wt.% of IL.

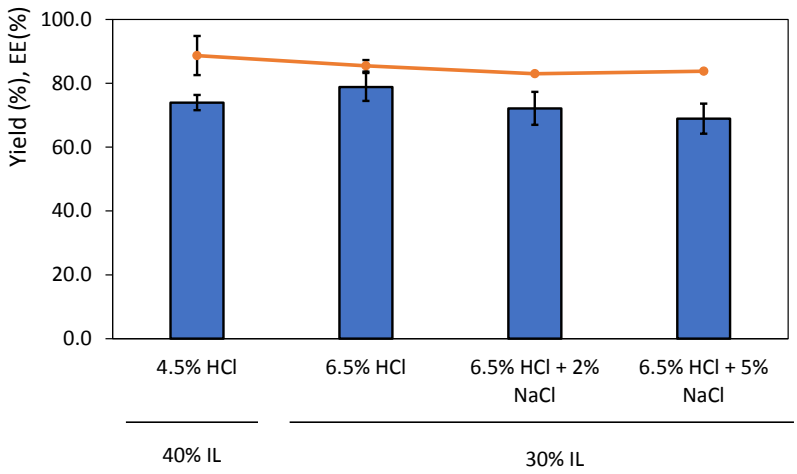

Figure S7. Furfural yield (bars) and extraction eficiency (dots) in the ABS. Assays were conducted at the fixed temperature of 140 °C. NaCl was added to the HCl concentration in the ABS.

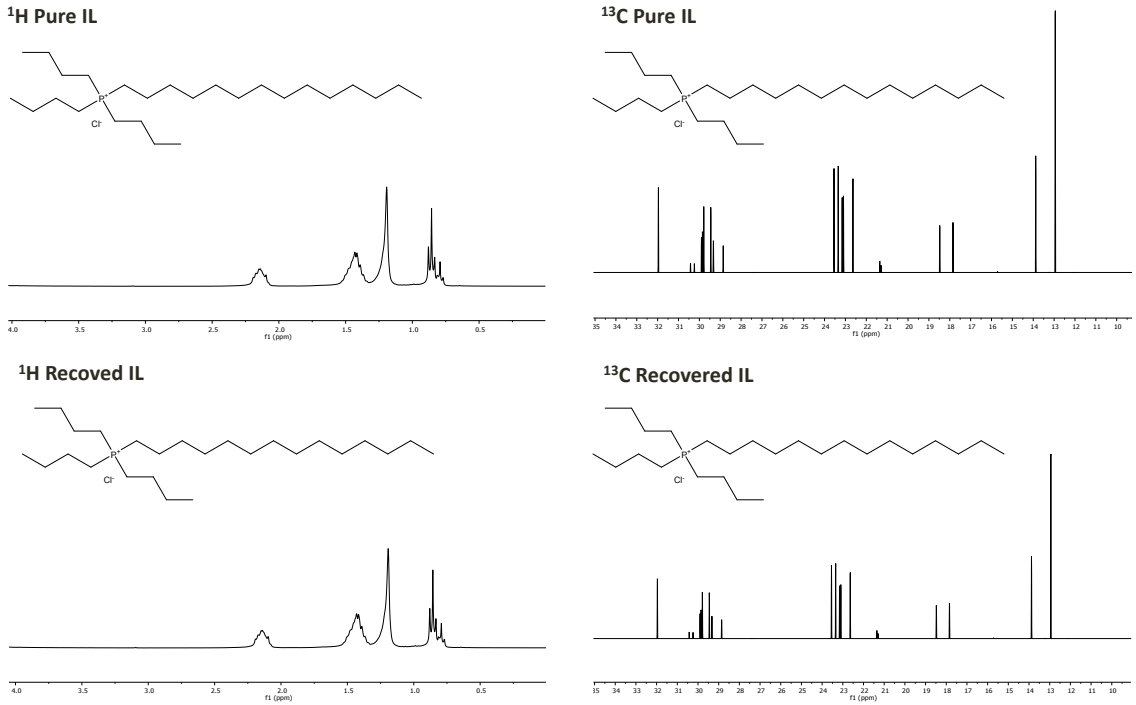

Figure S8. ^{1}H and ^{13}C NMR spectra of the pure and recovered IL.

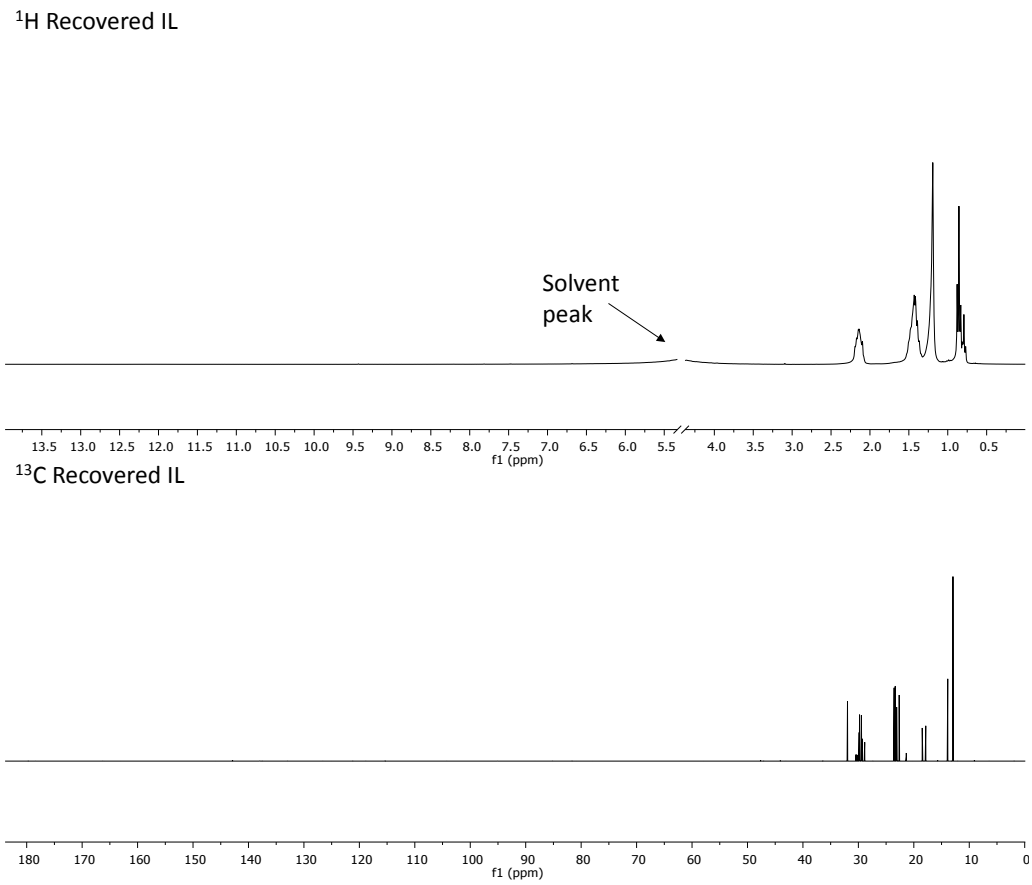

Figure S9. Full ^{1}H and ^{13}C NMR spectra of the recovered IL.

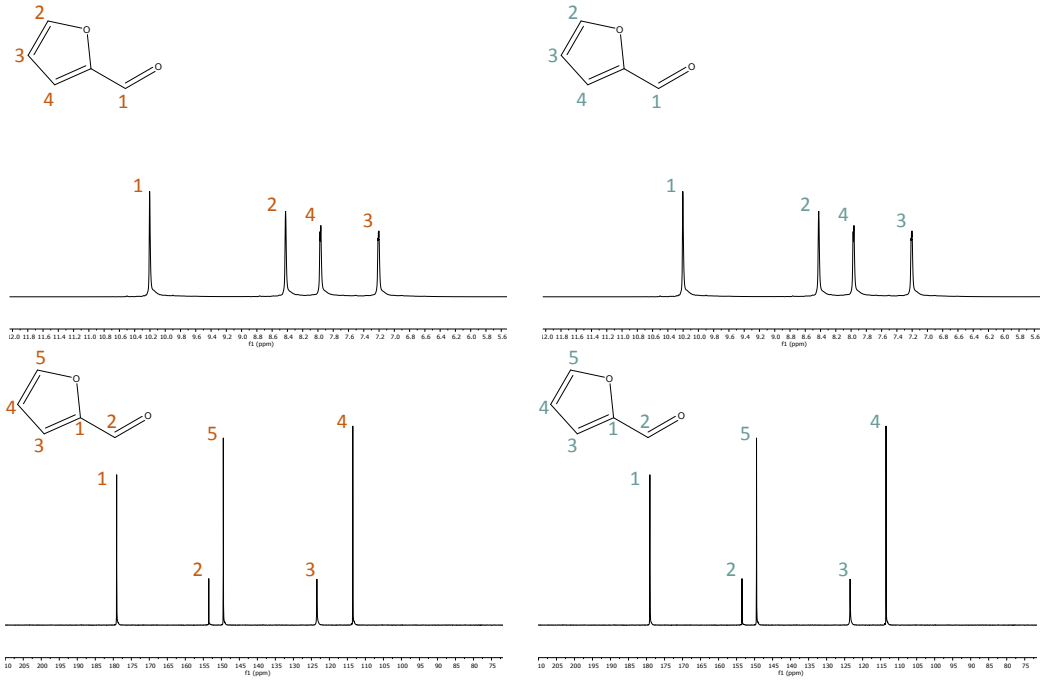

Figure S10. ^{1}H and ^{13}C NMR of standard (left) and recovered furfural (right).

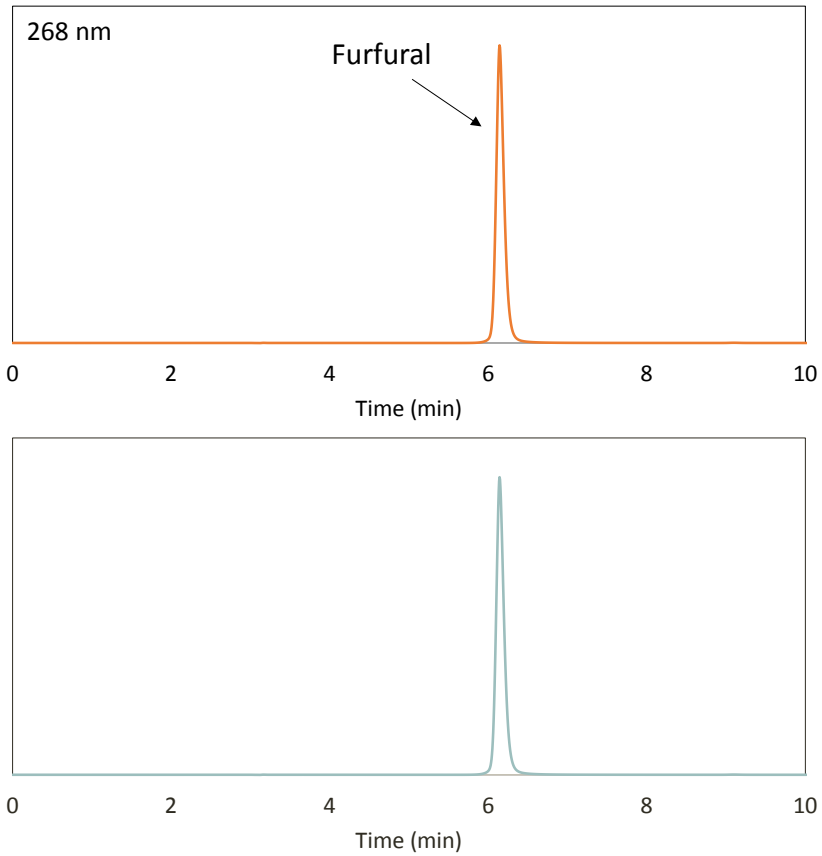

Figure S11. HPLC chromatogram at 268 nm of the standard (top) and recovered furfural (bottom).

References

(1) Khuri, A. I.; Mukhopadhyay, S. Response Surface Methodology. *Wiley Interdiscip. Rev. Comput. Stat.* **2010**, *2* (2), 128–149. https://doi.org/10.1002/wics.73.